ELSEVIER

Surface and Coatings Technology 156 (2002) 306–310

SURFACE & COATINGS TECHNOLOGY

www.elsevier.com/locate/surfcoat

Influence of ion and neutral flux on the properties of diamond-like carbon from pulsed glow discharges of acetylene

Kevin C. Walter, Michael Nastasi*

Materials Science and Technology Division, MS-K765, Los Alamos National Laboratory, Los Alamos, NM 87545, USA

Abstract

The deposition rates, composition and mechanical properties of diamond-like carbon (DLC) coatings deposited using pulsed glow discharges of acetylene (C_2H_2) have been studied as a function of deposition bias and gas pressure. The data show that a −4-kV bias is one order of magnitude more efficient than a bias of −8 kV for depositing DLC via plasma immersion ion processing (PIIP). Sputtering is the suspected cause for the reduced deposition efficiency at −8 kV. A methodology for comparing the magnitude of the ion and neutral flux is used to show that neutrals dominate the deposition process under all conditions tested. The necessary data are shown to prove that the coating hardness is independent of gas pressure when the ion flux, J_i, is less than 10% of the total flux, J_d. If J_i/J_d is greater than 10%, then increasing the gas pressure reduces the coating hardness to levels below 15 GPa. The implications of these results regarding sheath thickness, deposition rates and throughputs for large-area processing (many m^2) are discussed.

Keywords: Diamond-like carbon (DLC); Thin film; Hardness; Plasma deposition

1. Introduction

Deposition of tribologically important coatings, such as DLC, continues to be of interest to both the scientific and industrial communities. The use of PIIP, and other variations of pulsed plasma depositions, for the deposition of adherent DLC coatings have recently been reviewed [1]. While PIIP is easily used to deposit various kinds of DLC, the process is not yet optimized, even though attempts to simultaneously coat many m^2 have been successful [2,3]. The following experiments were performed for the purpose of determining optimum conditions for DLC deposition onto large and complicated surfaces.

2. Experimental details

All the DLC coatings evaluated in this work were deposited using the PIIP facility at Los Alamos National Laboratory [4]. The acetylene (C_2H_2) plasma was generated using a pulsed glow-discharge process, as this process is the most easily scaled to treat large areas (many m^2). The acetylene gas is referred to as 'welding grade,' and contains small amounts of acetone to prevent polymerization during storage. The coatings were deposited onto various substrates, but typically silicon, on an 840-cm^2 stage cooled with water at 20 °C. No attempt was made to measure the temperature of the sample or of the sample stage. The bias voltage was −4 and −8 kV, the pulse width ranged from 15 to 75 μs, the pulse frequency ranged from 0.6 to 4 kHz, and the C_2H_2 pressure ranged from 0.67 to 4 Pa (5 to 30 mtorr) (Table 1). The thickness of the coatings, which ranged from 60 nm to 1.3 μm, was measured using standard surface-contact profilometry. The chemical composition of the coatings was determined using standard Rutherford backscattering spectrometry and elastic recoil detection techniques [5]. The hardness and elastic modulus of the coatings were determined by nanoindentation. The results reported are an average of 6–10 individual measurements.

3. Results and discussion

The parameters measured and results from the coatings are listed in Tables 2 and 3. Fig. 1 shows the

*Corresponding author. Tel.: +1-505-667-7007; fax: +1-505-665-2992.

E-mail address: nasty@lanl.gov (M. Nastasi).

0257-8972/02/$ - see front matter
PII: S0257-8972(02)00095-6

Table 1
DLC deposition parameters of bias (V), gas pressure (P), pulse width (τ), frequency (f) and duty factor (F)

Run	V (kV)	P (Pa)	Pulse parameters		
			τ (μs)	f (kHz)	F
1	4	5	30	4	0.12
2	4	5	75	3.33	0.25
3	4	5	4	15	0.06
4	4	10	4	15	0.06
5	4	10	75	3.33	0.25
6	4	10	15	0.667	0.01
7	4	20	75	3.33	0.25
8	4	20	30	4	0.12
9	4	20	30	4	0.12
10	4	20	15	4	0.06
11	4	20	15	0.667	0.01
12	8	5	15	4	0.06
13	8	5	30	4	0.12
14	8	5	75	3.33	0.25
15	8	20	15	4	0.06
16	8	20	15	4	0.12
17	8	20	30	4	0.12
18	8	20	75	3.33	0.25

Table 3
Results of the hardness (H), elastic modulus (E), ion flux (J_i), neutral flux (J_d) and their ratio (J_i/J_d)

Run	H (GPa)	E (GPa)	Flux (10^{15} atoms cm^{-2} s^{-1})		J_i/J_d
			J_i	J_d	
1	15.3	156	0.02	0.65	0.03
2	15	151	0.07	1.53	0.05
3			0.05	0.38	0.14
4	17	150	0.31	2.22	0.14
5	17	150	0.54	2.88	0.19
6	17.5	171	0.74	3.00	0.25
7	15	120	0.01	2.38	0.05
8	17	140	0.30	7.25	0.04
9			0.02	0.33	0.07
10	12	120	0.89	12.20	0.07
11	13.5	120	0.57	7.50	0.08
12	17	130	0.62	7.75	0.08
13	16	120	0.40	5.35	0.08
14	17	150	0.08	1.82	0.04
15	8.5	94	1.25	5.78	0.22
16	12.2	124	1.78	4.67	0.38
17	6	85	1.78	5.67	0.31
18	13	162	4.46	12.90	0.35

results of deposition rate plotted against the average deposition power, $\langle P\rangle = \langle I_p\rangle Vf/A$, where $\langle I_p\rangle$ is the average current during the pulse, V is the pulse bias, f is the duty cycle and A is the stage area. The deposition rates vary from 0.07 to 3.9 μm h^{-1}. The lines are a linear fit through the data points for depositions at bias of -4 and -8 kV. The slopes of the -4- and -8-kV lines are 10.8 and 1.2 μm h-1 W^{-1} cm^2, respectively. It is speculated that the deposition rate for bias of -8 kV is reduced because of sputtering. The sputtering yield has a high dependence on energy [6], especially at the low ion energy values (<1 keV) expected when the operating pressure is high enough to account for numerous ion–neutral collisions in the sheath. Regardless of the reason, bias of -4 kV is approximately 10-fold more efficient than -8 kV. This result has positive

Table 2
A list of results, including the average current during a pulse ($\langle I_p\rangle$), the average power calculated ($\langle P\rangle$), the deposition rate (R), the coating thickness (t), and composition of the coating

Run	$\langle I_p\rangle$ (A)	$\langle P\rangle$ (W cm^{-2})	R (μm h^{-1})	t (μm)	[C] (at.%)	[H] (at.%)	[O] (at.%)
1	0.01	0.006	0.17	0.21	71	29	
2	0.02	0.024	0.34	0.50	66	34	
3	0.06	0.017	0.09	0.15	75.5	24.5	
4	0.12	0.034	0.55	0.56	68	32	
5	0.08	0.095	1.05	0.35	68	32	
6	0.16	0.008	0.07	0.06	70	30	
7	0.24	0.235	3.40	1.3	65	35	0.5
8	0.32	0.183	2.10	0.85	64.5	34.5	0.5
9	0.35	0.200	1.40	0.64	65	35	0.5
10	0.45	0.128	1.50	1.2	61.5	38.5	0.5
11	0.55	0.026	0.45	0.24	65.5	34.5	
12	0.35	0.200	0.54	0.27	68	31	1
13	0.3	0.342	0.98	0.25	72	28	
14	0.2	0.476	0.90	0.3	71	27	2
15	1.4	0.800	2.10	0.6	68	31	1
16	1.0	1.141	1.20	0.3	73	27	
17	1.0	1.141	1.68	0.42			
18	1.2	2.854	3.90	1.3	73.2	25.7	1

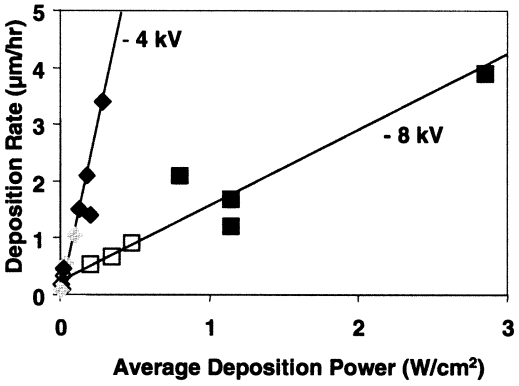

Fig. 1. Plot of deposition rates measured against the average deposition power for −4 kV (diamond symbols) and −8 kV (square symbols) bias. The open symbols are for data at 0.67 Pa (5 mtorr) of acetylene gas pressure. The gray symbols are for 1.3 Pa (10 mtorr), and the solid symbols are for 4 Pa (20 mtorr) of gas pressure.

implications for scaling up the deposition process, as a lower bias implies a smaller sheath, and thus higher packing density for components in a PIIP chamber, as discussed below.

The mechanical properties of the coatings are shown in Table 3 and Fig. 2. Note that $H/E=0.1$, as required for covalent solids [7], and that coating hardness ranges from 5 (equivalent to steel) to 25 GPa (equivalent to ceramics).

The hydrogen content [H] of the coatings is plotted against the coating hardness in Fig. 3 and listed in Table 3. Note that there is no clear dependence of hardness on H content. However, it can be said that the H content ranges between 20 and 40 at.%, as is typical for DLC coatings.

It is well known that not all of the material deposited from a plasma process is made up of ions. While it is difficult to directly measure the neutral flux onto a surface in a plasma environment, it is simpler to estimate the ion flux. The total amount of material deposited can also be calculated by combining the results of ion beam

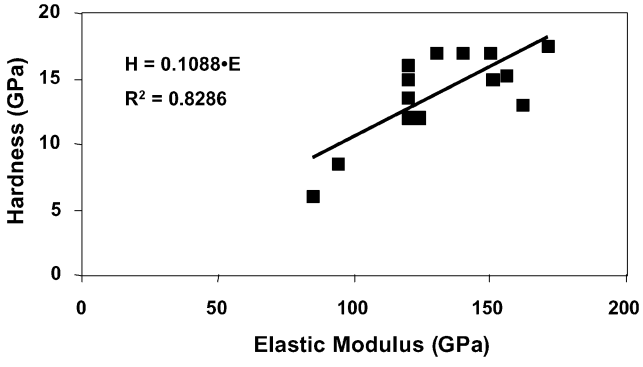

Fig. 2. Graph of hardness vs. elastic modulus of DLC coatings deposited by PIIP and measured by nanoindentation.

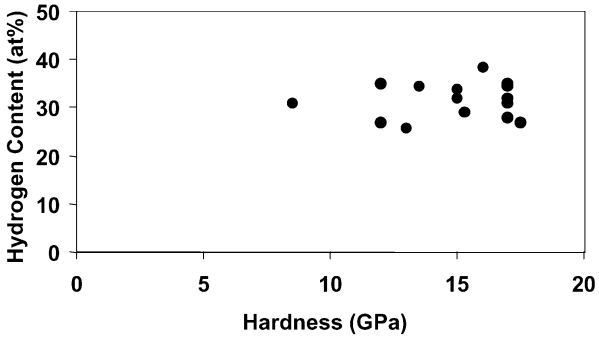

Fig. 3. Plot of [H] vs. coating hardness as measured by nanoindentation. The remainder of the coating composition is made up of carbon and trace amounts (<1 at.% of oxygen).

analysis. We define the ion flux, J_i, to be:

$$J_i = \frac{\langle I_p \rangle f \eta}{Ae}$$

where $\langle I_p \rangle$ is the average current during the pulse, f is the duty cycle, η is the number of carbon atoms per ion (assumed to be two for $C_2H_2^+$), A is the area being coated and e is the electronic charge. The average flux of material from both ions and neutrals, J_d, is calculated from:

$$J_d = \frac{(Nt)}{T} = J_i + J_n$$

where (Nt) is the atomic areal density measured from ion beam analysis, T is the total deposition time and J_n is the deposition flux due to neutral atoms and molecules that are not subsequently sputtered from the surface. A plot of J_d vs. J_i is shown in Fig. 4 and the values are listed in Table 3. Note that the trends in Fig. 4 are nearly identical to those shown in Fig. 1. This is not surprising, as the deposition rate is proportional to J_d

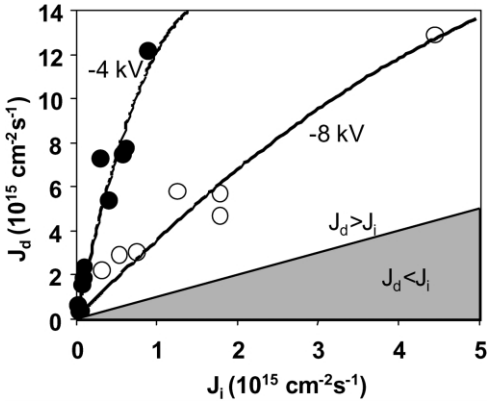

Fig. 4. Plot of the deposition rates (atoms cm^{-2} s^{-1}) for DLC deposited from PIIP at −4 and −8 kV of bias. The gray area represents a region where $J_d < J_i$ and resputtering would be the dominant process. The lines represent a polynomial fit to the data sets.

and the average deposition power is proportional to J_i. However, it is instructional to plot the data as in Fig. 4, because it makes the point that, in all cases, $J_d > J_i$, which indicates that neutrals always play a role in the deposition. In fact, J_d is always greater than $2J_i$, which means that deposition by neutrals, namely J_n, always dominates coating growth.

Regarding the mechanical properties of the DLC coatings, the coating hardness is essentially independent of the bias, duty factor and deposition rate. These plots are shown in Fig. 5.

Fig. 6 shows the dependence of DLC coating hardness on the J_i/J_d ratio. The hardness is practically independent of J_i/J_d when this ratio is less than 0.1. However, increasing the gas pressure when J_i/J_d is greater than 0.1 can decrease the hardness by approximately 50%.

These results have consequences for PIIP scale-up that should be carefully considered. For instance, a commercial operation would meet the following goals:

- Maximize the coating thickness per unit power consumed;
- Maximize the packing density of components; and
- Minimize the dependence on operational parameters (e.g. pressure and voltage).

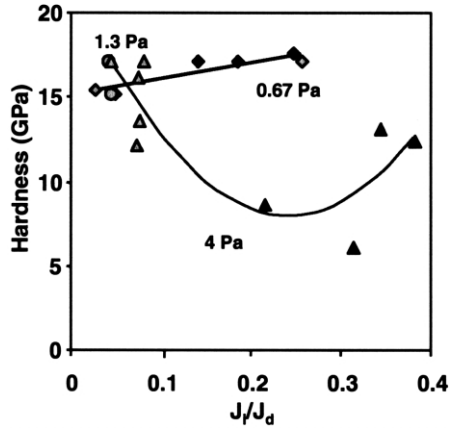

Fig. 6. Plot of DLC hardness vs. J_i/J_d and gas pressure. The gray symbols indicate a −4-kV bias and black, −8 kV. Triangles are used for 0.67 Pa (5 mtorr), circles for 1.3 Pa (10 mtorr) and triangles for 4 Pa (20 mtorr) of pressure.

From Fig. 1, the highest deposition rate utilizing the lowest power occurs for 4 Pa (20 mtorr) of gas pressure and a pulse bias of −4 kV. For the data presented in Fig. 5, the J_i/J_d ratio measured for the high-hardness DLC was less than 0.1, and these hardness properties

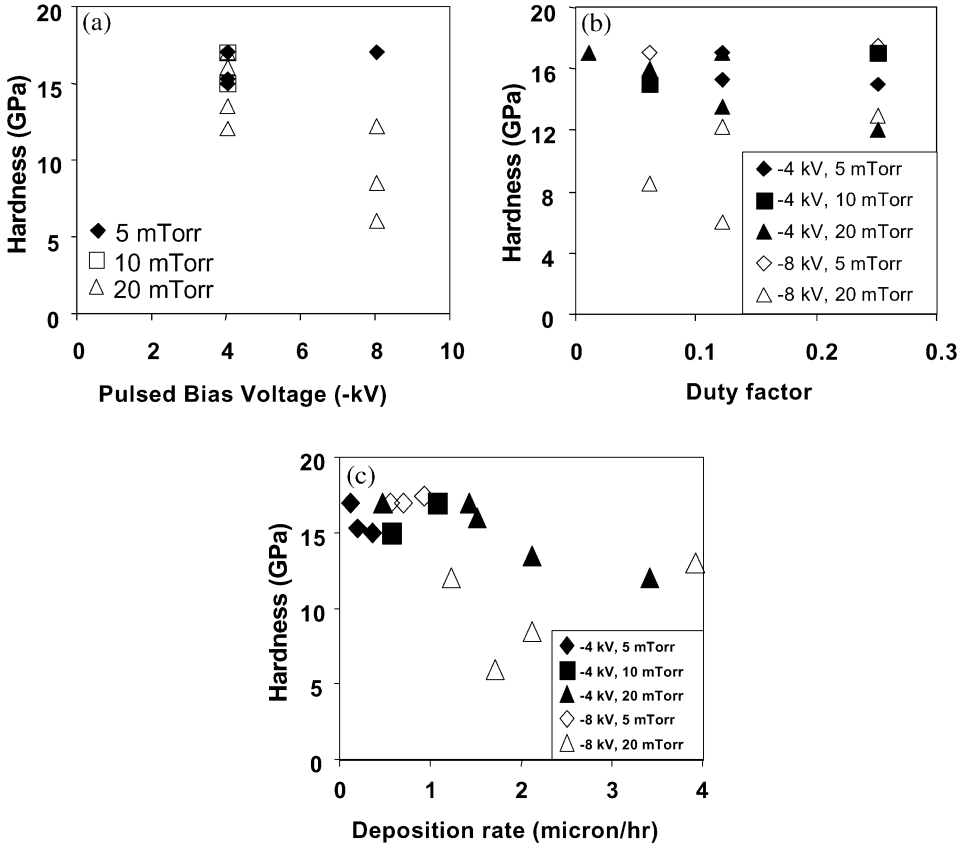

Fig. 5. Plots of: (a) coating hardness as a function of bias and acetylene pressure; (b) coating hardness as a function of duty factor, bias and pressure; and (c) coating hardness as function of deposition rate.

experimentally appear to be independent of variations in bias and pressure for the present set of experimental conditions. The packing density of components is maximized when the sheath thickness is minimized. The sheath thickness is proportional to $(V/n)^{1/2}$ and the pulse width, τ; thus, using a lower bias, a higher ion density (or gas pressure) and a shorter pulse width will minimize the extent of a sheath. Assuming an ion density of 10^9 cm^{-3} and a $C_2H_2^+$ ion, the sheath thickness calculated for bias of -4 and -8 kV is 9 and 13 cm, respectively, for a 15-μs pulse.

4. Summary and conclusions

DLC coatings deposited via pulsed glow discharges of acetylene have been compared as a function of bias, pressure and duty cycle. The most efficient process parameters are -4 V, 4 Pa (20 mtorr) of pressure, and a duty cycle between 0.05 and 0.1. Under these conditions, components can be as little as 18 cm (twice the sheath thickness) apart. The DLC coatings are deposited at rates of up to 3 μm h^{-1} and have a hardness of approximately 15 GPa.

There is no obvious relationship between the coating hardness and a combination of process parameters (e.g. pressure, bias, or duty factor). There is obviously another parameter that is not accounted for in the preceding analysis. While the gas composition is constant (acetylene), perhaps the ion and/or neutral species change drastically within the parameter ranges reported. Indeed, qualitative comparisons of residual gas analysis (RGA) spectra taken during each deposition experiment show no change with bias or duty factor, but do show an increase in the concentration of particles with mass 2 and 50 a.m.u. Molecular hydrogen is likely responsible for the signal at 2 a.m.u., and some polymeric combination of carbon and hydrogen are responsible for the signal at 50 a.m.u. (i.e. C_4H_2 radical, C_4H_4 and derivatives). The increase in concentration of these particles weakly correlates with a decrease in the coating hardness.

While the sample stage was actively cooled with 20 °C water, the temperature of the sample stage was not measured and could have varied, especially when using a -8-kV bias. The effect of temperature on DLC properties, especially hardness, is complicated, but could be responsible for the increase in hardness using -8 kV and 4 Pa (20 mtorr) as observed in Fig. 6.

Acknowledgments

This work was supported by the DOE Office of Science.

References

[1] A. Anders (Ed.), Handbook of Plasma Immersion Ion Implantation and Deposition, John Wiley & Sons, New York, 2000, pp. 569–573 (and references therein).
[2] B.P. Cluggish, C.P. Munson, J. Appl. Phys. 84 (1998) 5937–5944.
[3] B.P. Cluggish, C.P. Munson, J. Appl. Phys. 84 (1998) 5944–5955.
[4] K.C. Walter, M. Nastasi, C. Munson, Surf. Coat. Technol. 93 (1997) 287.
[5] J.R. Tesmer, M. Nastasi (Eds.), Handbook of Modern Ion Beam Materials Analysis, Materials Research Society, Pittsburgh, PA, 1995.
[6] M. Nastasi, J.W. Mayer, J.K. Hirvonen, Ion–Solid Interactions: Fundamentals and Applications, Cambridge University Press, New York, 1996, pp. 223–227.
[7] J. Robertson, Prog. Solid-State Chem. 21 (1991) 199.